

ChemComm

Accepted Manuscript



This is an *Accepted Manuscript*, which has been through the Royal Society of Chemistry peer review process and has been accepted for publication.

Accepted Manuscripts are published online shortly after acceptance, before technical editing, formatting and proof reading. Using this free service, authors can make their results available to the community, in citable form, before we publish the edited article. We will replace this *Accepted Manuscript* with the edited and formatted *Advance Article* as soon as it is available.

You can find more information about *Accepted Manuscripts* in the [Information for Authors](#).

Please note that technical editing may introduce minor changes to the text and/or graphics, which may alter content. The journal's standard [Terms & Conditions](#) and the [Ethical guidelines](#) still apply. In no event shall the Royal Society of Chemistry be held responsible for any errors or omissions in this *Accepted Manuscript* or any consequences arising from the use of any information it contains.



Journal Name

COMMUNICATION

H-Bonding and Charging Mediated Aggregation and Emission for Fluorescence Turn-on Detection of Hydrazine Hydrate

Received 00th January 20xx,
Accepted 00th January 20xx

Deyan Zhou,[†] Yangyang Wang,^{†,‡} Jiong Jia,[†] Wenzhu Yu,[†] Baofeng Qu,[†] Xia Li,[†] Xuan Sun^{†*}

DOI: 10.1039/x0xx00000x
www.rsc.org/

In situ morphological transition and turn-on fluorescence of self-assembly of NDI derivative driven by hydrazine hydrate are realized through H-bonding and charging of the aromatic building blocks, demonstrating a stimuli-responsive supramolecular system to be useful for visual detection of hydrazine hydrate.

One of the important goals of supramolecular chemistry is to develop the externally controlled systems, that is, the structure or other physical properties of the well-defined molecular aggregates or supramolecules can be changed or switched in a predictable manner by an external signal. The key to a successful switch is that the external signal strongly perturbs an important binding interaction holding together the supramolecular complex. As exploited in nature, H-bonding (HB) with the highly directional nature is envisioned essential to govern and modulate the structure and morphology of the artificial supramolecular architecture by precise defining the spatial organization of the building blocks in the self-assembled state. Specifically, through regulation of electronic states, HB mediated supramolecular assemblies of photophysically rich π -conjugated chromophores provides an exciting opportunity for fine tuning the functions of the assemblies such as luminescence characteristics¹ or transport properties, as sensing²⁻⁴ and molecular electronics.⁵⁻⁷ Charging of an aromatic primary building block is also evidenced to be an effective way for controlling the structure of the supramolecular assemblies⁸. The bisimides, having an aromatic core such as naphthalenediimides (NDIs) or perylenediimides (PDIs) are intriguing n-type building blocks to fabricate specific aggregated structures with semiconductivity⁹⁻¹² or photoluminescence^{13,14}. Through reversible charging of the PDI moieties, the initially obtained long fibers from the self-organized PDIs underwent reversible fission, accompanied by a significant change in electronic properties, which is envisaged for adaptive photo-function

switching⁸. The in situ control over self-assembly and photo-function of aromatic building blocks, such as PDIs and NDIs, arise from the ease of reversible reduction and color change between the three redox states (neutral, radical anion, and dianion). The production of radical anions of the NDI in aqueous solution is feasibly achieved by chemical reduction, rendering it colorimetric sensors for detection of F⁻¹⁵⁻¹⁷, CN⁻¹⁸, or amines¹⁹. However, there is much less information available on the aggregates of NDI radical anions, in spite of its central role in electron- and energy-transfer systems²⁰⁻²³.

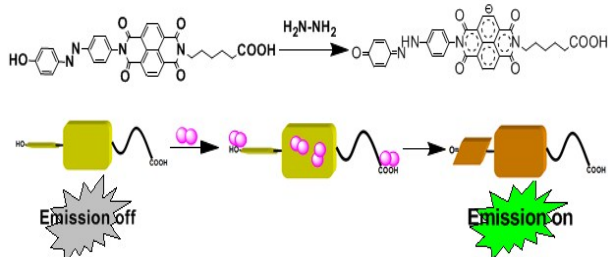
As a class of important chemicals, hydrazine is valuable in many fields but has toxicity, the detection is therefore quite essential.²⁴⁻²⁸ Hydrazine contains two amino groups, and it can easily form extended arrays of HB (NH⁺...O and NH⁺...N), which may be particularly interesting for modulation of molecular assembly through HB. Detection of hydrazine hydrate by an Au nanoparticles-based colorimetric sensing system was realized based on HB recognition²⁹. Meanwhile, hydrazine is strong reductant that can potentially reduce the aromatic electron-withdrawing chromophores to form radical ions with characteristic spectroscopic signatures. Adding hydrazine into a supramolecular assembly system may trigger the reduction of the aromatic building blocks and mediate both morphology and photo-function of the assembly by HB and charging, which may be considered as a novel strategy for design of hydrazine probes. As an important probe technique, fluorescence turn-on detection is advantageous because of its high sensitivity and easy-operation.³⁰⁻³⁴ Specifically, fluorescence turn-on detection based on aggregation modulation was rarely reported. Herein we report on hydrazine modulated morphological transformation and turn-on fluorescence of self-assembled nanoribbons. A nearly non-fluorescent host dyad **NDI-AB 1** (Scheme 1) is constructed by introducing an electron-donating moiety azobenzene (AB) to the potential fluorophore NDI. As expected, **1** is non-planar, as the result of the sterically demanding framework exhibiting weak fluorescence yielding mainly from twisted intramolecular charge transfer (TICT) effect.^{33,35} In water, **1** self-assembled into well-ordered nanoribbons with further fluorescence

[†]Key Laboratory for Colloid & Interface Chemistry, Shandong University, Education Ministry, Jinan, 250100, P. R. China

[‡]State Key Lab of Crystal Materials, Shandong University, Jinan, 250100, P. R. China
E-mail: sunxuan@sdu.edu.cn

Electronic Supplementary Information (ESI) available: [Experimental procedures, characterization data, and additional spectra.]. See DOI: 10.1039/x0xx00000x

quenching by π - π interaction. Upon addition of hydrazine hydrate, interactions between aromatic monomers were attenuated by HB intervention and the reduction to anionic species, which causes ribbons fission accompanied by a remarkably enhanced emission from the aggregated radicals.



Scheme 1. Schematic illustration of the reaction of molecule **1** with hydrazine hydrate.

Dyad **1** was readily synthesized by one-step reaction between the respective azobenzene derivative and naphthaleneimide, and fully characterized using ^1H NMR, ^{13}C NMR and mass spectra (Scheme S1, ESI $^+$). The control compounds **COOH-NDI 2** and **OH-AB 3** were also synthesized and characterized, respectively (Scheme S2 and S3 ESI $^+$). **1** is well dissolved in DMSO, showing essentially a superposition of absorptions of **2** and **3** (Fig. S1a, ESI $^+$), dominated by a typical strong π - π^* transition of the NDI model with vibronically split peaks (Fig. 1). Fluorescence study of **1** in DMSO reveals broad emission with rather weak quantum yield of $\Phi_{\text{PL}} = 2.37\%$, which is quenched with respect to **2** (Fig. 1 and S1b, ESI $^+$). The electrochemical behavior of **1** (Fig. S2, ESI $^+$) showed two well-separated, reversible one-electron reduction waves corresponding to the formation of the radical anion and dianion, respectively, which are more negative owing to the electron donating effect of the AB moiety¹⁵.

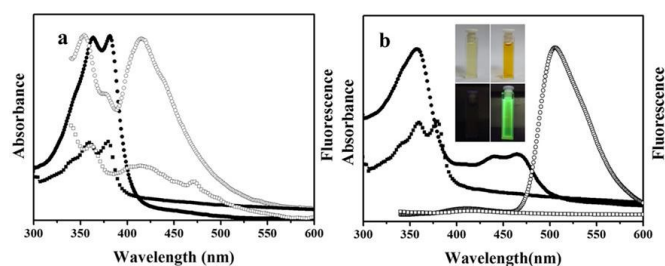


Fig. 1 (a) UV-vis absorption spectra of molecule **1** in DMSO (25 μM , \bullet) and the aggregates (\blacksquare), and normalized fluorescence spectra of molecule **1** in DMSO (25 μM , \circ) and the aggregates (\square); (b) UV-vis absorption spectra of aggregates in water before (\blacksquare) and after (\bullet) adding hydrazine hydrate, and normalized fluorescence spectra of aggregates in water before (\square) and after (\circ) adding hydrazine hydrate, inset is the photographical images of the aggregates before (left) and after (right) adding hydrazine hydrate.

In water, molecule **1** gradually self-assembled into 1-D nanoribbons with high aspect ratio as observed by transmission

electron microscopy (TEM, Fig. S3a, ESI $^+$) and confocal fluorescence microscopy (CFM, Fig. 2a and 2b). The UV/vis spectroscopy of the nanoribbons in water shows hypochromic effect with respect to that of the molecular absorption of **1** in DMSO (Fig. 1a). Meanwhile, the fluorescence of the nanoribbons further attenuates relative to that of the monomeric compound (Fig. 1b). Combined with the broad absorption of O-H stretching vibration at 3300-3500 cm^{-1} in solid state FT-IR spectra (Fig. S4a, ESI $^+$) and the π -stacking signal in the wide-angle XRD pattern (Fig. S5, ESI $^+$) of the nanoribbons, it demonstrates that highly ordered H-aggregation is provided by synergy between the π - π stacking and intermolecular H-bonding.

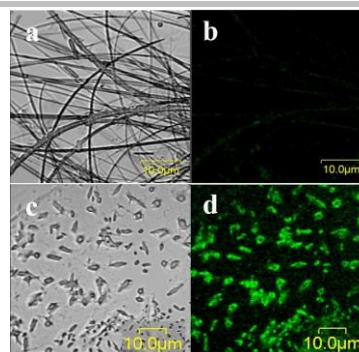


Fig. 2 CFM images of the aggregates of **1** (a, b) before and (c, d) after adding hydrazine hydrate.

Firstly, we investigated the interactions between the molecule **1** and hydrazine in DMSO followed by absorption and fluorescence spectra. All the spectra were acquired instantly after adding hydrazine (within 5s). From the variation in the absorption spectra (Fig. 3a) with increasing concentrations of hydrazine, a two-step reaction is deduced that involved between **1** and hydrazine. Upon addition of hydrazine, a relatively broad absorption band with maximum at 500 nm arose promptly accompanied with the attenuation of the NDI absorption. The intensity of this new absorption band increased along with increasing the hydrazine concentrations, then declined with further addition of hydrazine. Meanwhile, a new sharp absorption band with maximum at 475 nm appeared, referring to the typical absorption of the NDI $^{\bullet-}$ (Fig. S6a, ESI $^+$)¹⁵⁻¹⁸. Compared with the azobenzene **3**, which demonstrated remarkable changes in the absorption spectra upon addition of hydrazine (Fig. S6b, ESI $^+$), the broad absorption at 500 nm may be ascribed to the azo-hydrazone tautomerism, which is interesting and supposed to exist in the dynamic equilibrium in an azophenone system^{36,37}. The presence of the -OH group is conducive to prompt the tautomerism to the hydrazone form and quinone structure at the presence of hydrazine (Scheme 1). Meanwhile, the electron-deficient NDI moiety was inclined to bind with hydrazine, and was feasibly reduced to the radical anion. In fact, these two step reactions may happen simultaneously as deduced from the absorption of NDI $^{\bullet-}$ at 600 nm (inset in Fig. 3a). When adding less than 5 equiv of hydrazine, absorption of NDI $^{\bullet-}$ can be observed indicating a relatively facile reduction process. ^1H NMR spectra of

the hydrazine addition products (Fig. S7, ESI[†]) well evidenced the formation of the quinone structure and NDI^{•-} radical by the significant peaks shift corresponding to the protons on AB unit and the disappearance of the signals of aromatic protons on NDI, respectively. Electron paramagnetic resonance (EPR) spectra manifested the formation of a delocalized NDI^{•-} radical anion¹⁶ at the presence of hydrazine. (Fig. S8, ESI[†]). Accompany with this two-step reaction, color change was generated sharply from yellow to deep-orange, as can be observed by naked eyes (Fig. 3a). The absorption of the dianion of NDI was not observed with further addition of hydrazine.

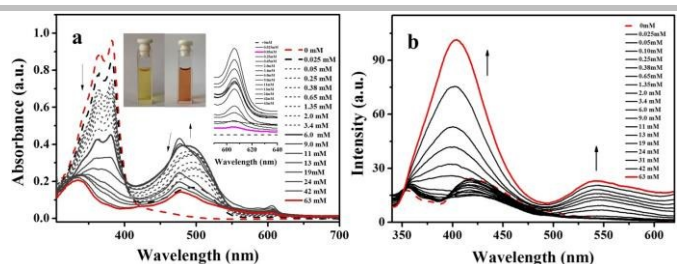


Fig. 3 (a) UV-vis absorption spectra and (b) fluorescence spectra of molecule **1** in DMSO (25 μ M) with addition of hydrazine.

With addition of hydrazine hydrate, fluorescence at 405 nm emitted from NDI was greatly enhanced as shown in Fig. 3b. Meanwhile, a new broad emission emerged in the longer wavelength region (500 – 600 nm). According to the excitation of **1** in DMSO at the presence of hydrazine (Fig. S9a, ESI[†]), this emission band was contributed together from the NDI unit and its radical anion NDI^{•-}, which has never been investigated in previous work. The “turn-on” fluorescence may refer to the TICT mechanism, where hydrazine induced hydrazone and quinone structures restrain the formation of the TICT state, directly leading to emission recovery (Scheme 1). Time-dependent density functional theory (TDDFT) calculations were carried out to elucidate the effect of steric hindrance on the fluorescence of **1** (Fig. S10, ESI[†]). This emission was sensitive to hydrazine, while in contrast, upon addition of a variety of other related test species, such as phenyl hydrazine, ethylenediamine, ammonium hydroxide, hydroxylamine hydrochloride, F⁻, I⁻, S²⁻, and SO₃²⁻, etc., only a fluorescence quenching at 420 nm or an insignificant change was observed, indicating the selectivity and specificity of **1** for hydrazine. (Fig. S11, ESI[†])

We then carried out experiments to check the effect of the hydrazine on the molecular aggregation. After adding hydrazine hydrate into the nanoribbons suspended in water, hyperchromic effect in the higher energy region (300 – 400 nm, Fig. 1b and Fig. S12a, ESI[†]) was displayed, corresponding to electronic transition of NDI moiety, which may indicate the nanoribbons fission. Meanwhile, a relatively weak absorption appeared in the lower energy region, which may relate to the absorption of NDI^{•-}. The fission of the nanoribbons was evidenced by TEM (Fig. S3b, ESI[†]) and CFM (Fig. 2c and 2d), revealing formation of nanovesicles with inhomogeneous

dimension, which was not sufficiently stable for XRD studies. Concerning the favor of formation of the H-bond and the strong reductive ability of the hydrazine hydrate, the morphological transition from nanoribbons to nanovesicles was envisaged to be modulated by synergetic H-bonding and charging effects. The absorption peaks of C=O on –COOH and amide in the FT-IR shifted to lower wave numbers after adding hydrazine hydrate, which clearly evidenced the H-bonding mediated structure transition (Fig. S4b, ESI[†]). Interestingly, the nanovesicles demonstrated an extremely strong green emission located at 500 nm (Fig. 1b and 2d), originating from both the NDI and NDI^{•-} radicals (Fig. S9b, ESI[†]) while the local emission from the NDI moieties at 400 nm as observed in DMSO solution was suppressed completely (Fig. S12, ESI[†]). When using F⁻ as the reductant, which was generally applied to reduce the bisimide aromatic molecules^{15–17}, neither the obvious morphological changes nor the fluorescence enhancement was observed (Fig. S11, ESI[†]). This diversity from the hydrazine hydrate revealed the synergetic effects of H-bonding and charging in modulating the assembly and the photo-function. The H-bond formation between hydrazine and the –COOH and/or –OH groups within the assembly of **1** greatly promoted the ability of **1** to trap hydrazine, which then facilitated the reduction of **1**. Meanwhile, H-bonding together with the higher electron density on the radical interrupted π -stacking between the molecules, finally leading to the fission of the nanoribbons and formation of the nanovesicles. Also, the aggregation transformation of **1** toward hydrazine hydrate was much more sensitive than that of the control compound **2** (Fig. S12, ESI[†]). The much higher fluorescence quantum yield ($\Phi_f = 14.98\%$) of the nanovesicles in water compared with that of single molecule in DMSO indicates the more stabilized radical anions in the aggregates. Moreover, such highly emissive nature brought bright green color of the aggregates suspension (Fig. 2d), which can be easily observed by naked-eye and would be beneficial for sensing. Therefore, the present system may be potentially useful for the detection of hydrazine.

In summary, we report facily in situ mediated self-assembly and photo-function of an aromatic building block **AB-NDI** by synergetic effect of H-bonding and charging of aromatic system. The emission of the radical anion and that from the radicals in the aggregation was studied for the first time. **AB-NDI** has been designed according to the TICT mechanism, which exhibited “turn-on” fluorescence response toward hydrazine. Aggregation reconstruction drove by hydrazine through H-bonding and charging exhibited extremely strong turn-on fluorescence, which is expected to be excellent sensors for hydrazine detection. We envisage that this methodology can be useful for the creation of adaptive multifunctional supramolecular systems.

This work was financially supported by NSFC (21371109) and the “Taishan Scholar” project of Shandong Province.

Notes and references

- 1 M. R. Molla, D. Gehrig, L. Roy, V. Kamm, A. Paul, F. Laquai and S. Ghosh, *Chem. Eur. J.*, 2014, **20**, 760.
- 2 N. H. Evans and P. D. Beer, *Angew. Chem. Int. Ed.*, 2014, **53**, 11716.
- 3 B. Gole, W. Song, M. Lackinger and P. S. Mukherjee, *Chem. Eur. J.*, 2014, **20**, 13662.
- 4 J. S. Chen, P. W. Zhou, G. Y. Li, T. S. Chu and G. Z. He, *J. Phys. Chem. B*, 2013, **117**, 5212.
- 5 A. Ueda, S. Yamada, T. Isono, H. Kamo, A. Nakao, R. Kumai, H. Nakao, Y. Murakami, K. Yamamoto, Y. Nishio and H. Mori, *J. Am. Chem. Soc.*, 2014, **136**, 12184.
- 6 S. S. Babu, S. Prasanthkumar and A. Ajayaghosh, *Angew. Chem. Int. Ed.*, 2012, **51**, 1766.
- 7 Y. Wang, D. Zhou, H. Li, R. Li, Y. Zhong, X. Sun and X. Sun, *J. Mater. Chem. C*, 2014, **2**, 6402.
- 8 J. Baram, E. Shirman, N. Ben-Shitrit, A. Ustinov, H. Weissman, I. Pinkas, S. G. Wolf and B. Rybtchinski, *J. Am. Chem. Soc.*, 2008, **130**, 14966.
- 9 H. Usta, A. Facchetti, and T. J. Marks, *Acc. Chem. Res.*, 2011, **44**, 501.
- 10 M. Gsänger, J. H. Oh, M. Könemann, H. W. Höffken, A.-M. Krause, Z. Bao, and F. Würthner, *Angew. Chem. Int. Ed.*, 2010, **49**, 740.
- 11 R. Schmidt, J. H. Oh, Y. Sun, M. Deppisch, A.-M. Krause, K. Radacki, H. Braunschweig, M. Könemann, P. Erk, Z. Bao, and F. Würthner, *J. Am. Chem. Soc.*, 2009, **131**, 6215.
- 12 L. Ma, J. Jia, T. Yang, G. Yin, Y. Liu, X. Sun and X. Tao, *RSC Adv.*, 2012, **2**, 2902.
- 13 M. R. Molla and S. Ghosh, *Chem. Eur. J.*, 2012, **18**, 1290.
- 14 M. R. Molla, D. Gehrig, L. Roy, V. Kamm, A. Paul, F. Laquai, and S. Ghosh, *Chem. Eur. J.*, 2014, **20**, 760.
- 15 S. Guha, F. S. Goodson, S. Roy, L. J. Corson, C. A. Gravenmier and S. Saha, *J. Am. Chem. Soc.*, 2011, **133**, 15256.
- 16 S. Guha and S. Saha, *J. Am. Chem. Soc.*, 2010, **132**, 17674.
- 17 S. Guha, F. S. Goodson, L. J. Corson and S. Saha, *J. Am. Chem. Soc.*, 2012, **134**, 13679.
- 18 M. R. Ajayakumar, P. Mukhopadhyay, S. Yadav and S. Ghosh, *Org. Lett.*, 2010, **12**, 2646.
- 19 M. R. Ajayakumar and P. Mukhopadhyay, *Chem. Commun.*, 2009, **25**, 3702.
- 20 J. Zheng, W. Qiao, X. Wan, J. P. Gao and Z. Y. Wang, *Chem. Mater.*, 2008, **20**, 6163.
- 21 N. Sakai, J. Mareda, E. Vauthey and S. Matile, *Chem. Commun.*, 2010, **46**, 4225.
- 22 S. V. Bhosale, C. H. Jani and S. J. Langford, *Chem. Soc. Rev.*, 2008, **37**, 331.
- 23 B. A. Jones, A. Facchetti, M. R. Wasielewski and T. J. Marks, *J. Am. Chem. Soc.*, 2007, **129**, 15259.
- 24 C. Hu, W. Sun, J. Cao, P. Gao, J. Wang, J. Fan, F. Song, S. Sun and X. Peng, *Org. Lett.*, 2013, **15**, 4022.
- 25 S. Goswami, S. Das, K. Aich, B. Pakhira, S. Panja, S. K. Mukherjee and S. Sarkar, *Org. Lett.*, 2013, **15**, 5412.
- 26 M. H. Lee, B. Yoon, J. S. Kim and J. L. Sessler, *Chem. Sci.*, 2013, **4**, 4121.
- 27 S. Goswami, K. Aich, S. Das, S. Basu Roy, B. Pakhira and S. Sarkar, *RSC Adv.*, 2014, **4**, 14210.
- 28 S. Goswami, S. Das, K. Aich, D. Sarkar and T. K. Mondal, *Tetrahedron Letters*, 2014, **55**, 2695.
- 29 Z. Zhao, G. Zhang, Y. Gao, X. Yang and Y. Li, *Chem. Commun.*, 2011, **47**, 12816.
- 30 Y. Ding, Y. Tang, W. Zhu and Y. Xie, *Chem. Soc. Rev.*, 2015, **44**, 1101.
- 31 Y. Xie, P. Wei, X. Li, T. Hong, K. Zhang and H. Furuta, *J. Am. Chem. Soc.*, 2013, **135**, 19119.
- 32 B. P. Biswal, S. Chandra, S. Kandambeth, B. Lukose, T. Heir and R. Banerjee, *J. Org. Chem.*, 2013, **135**, 5328.
- 33 B. Chen, Y. Ding, X. Li, W. Zhu, J. P. Hill, K. Ariga and Y. Xi, *Chem. Commun.*, 2013, **49**, 10136.
- 34 B. Chen, X. Sun, X. Li, H. Ågren and Y. Xie, *Sensors and Actuators B: Chemical*, 2014, **199**, 93.
- 35 Z. R. Grabowski and K. Rotkiewicz, *Chem. Rev.*, 2003, **103**, 3899.
- 36 J. M. Saveant and C. Tard, *J. Am. Chem. Soc.*, 2014, **136**, 8907.
- 37 X. Chen T. Tao, Y. Wang, Y. Peng, W. Huang and H. C., *Dalton Trans.*, 2012, **41**, 11107.
- 38 The fluorescence quantum yield should be much higher than 14.98% since the strong irradiation applied for measurement severely quenched the emission by annihilating the radical ions.